Carbohydrate Polymers 220 (2019) 110–117

Contents lists available at ScienceDirect

Carbohydrate Polymers

journal homepage: www.elsevier.com/locate/carbpol

Enzymatically assisted isolation of high-quality cellulose nanoparticles from water hyacinth stems

Gregorio N. Juárez-Luna[a], Ernesto Favela-Torres[a], Iván R. Quevedo[b], Nikola Batina[c,*]

[a] Departamento de Biotecnología, CBS, Universidad Autónoma Metropolitana – Iztapalapa (UAM-I), Av. San Rafael Atlixco 186, Col. Vicentina, Del. Iztapalapa, C.P. 09340, Ciudad de México, México

[b] Departamento de Ingeniería Química Industrial y de Alimentos (DIQIA), Universidad Iberoamericana Ciudad de México (UIA). Prolongación Paseo de la Reforma 880, Santa Fe, Col, Contadero, C.P. 01219, Ciudad de México, México

[c] Laboratorio de Nanotecnología e Ingeniería Molecular, Departamento de Química, CBI, UAM-I, Av. San Rafael Atlixco No. 186, Col. Vicentina, Del. Iztapalapa, C.P. 09340, Ciudad de México, México

ARTICLE INFO

Keywords:
Cellulose nanoparticles
Cellulose nanocrystals
Cellulase complex
Water hyacinth stems
Enzymatic hydrolysis
AFM
XRD

ABSTRACT

High quality cellulose nanoparticles (CNP) were isolated from water hyacinth stem cellulose (Cel-WH) extracted via successive thermochemical and alkaline-peroxide treatments, and further enzymatically hydrolysed using the commercial cellulase complex, NS22086, at 50°C. The maximum CNP concentration was reached after 120 min of enzymatic hydrolysis, with a hydrodynamic diameter in the order of 200 − 250 nm and an increase of 5% in crystallinity as compared with Cel-WH. The obtained rod-shaped cellulose nanocrystals, as revealed by atomic force microscopy (AFM), exhibited a nominal diameter of 15.6 − 29.4 nm, a length of 56 − 184.8 nm, and a height of 2.85 − 6.43 nm, indicating a low tendency to form aggregates. In the present study, it was found that water hyacinth stems are a valuable source for the isolation of high-quality CNP using an environmentally friendly procedure, with potential applications in nanomedicine and nanopharmacology.

1. Introduction

The high reliance on non-sustainable practices has led to an economic and environmental crisis in our society; making a priority the development of products derived from renewable biomass, mainly lignocellulosic materials from industrial and agricultural activities (Chen, Deng, Shen, & Jiang, 2012). Water hyacinth (*Eichhornia crassipes*) is a noxious weed that has attracted worldwide attention due to its fast-spread and crowded growth, which leads to serious unfavourable effects on the environment, human health, and economic development. Moreover, vast amounts of money have been spent to selectively remove it from water bodies (Rezania et al., 2015). This plant contains up to 60% cellulose (Abdel-Fattah & Abdel-Naby, 2012; Rezania et al., 2015; Sindhu et al., 2017). Cellulose has been used in a broad range of applications, since it is highly available, biodegradable, biocompatible, and can be isolated in the form of nanoparticles, making it an attractive material for study (Boluk & Danumah, 2014).

Cellulose nanoparticles (CNP) usually appear as rod-like or ribbon-like particles, the length of which typically ranges from 50 to 1000 nm and the diameter fluctuates between 3 and 50 nm (Kaushik & Moores, 2016). Due to their nanometric scale, CNP exhibit physicochemical properties such as a low density (1.6 g cm^{-3}), low thermal expansion coefficient (10^{-7} K^{-1} in the longitudinal direction), high Young's modulus (138 GPa in the crystal region along the longitudinal axis), and high tensile strength (Abe, Iwamoto, & Yano, 2007; Fattahi Meyabadi, Dadashian, Mir Mohamad Sadeghi, & Ebrahimi Zanjani Asl, 2014). These properties make CNP an ideal candidate for novel applications such as high performance nanocomposites (i.e., reinforcing fibres), filtration media, paints and coatings, and personal care, in addition to biomedical, hygiene, and absorbent products (Boluk & Danumah, 2014).

Isolation of CNP from lignocellulosic biomass can be accomplished by induced destruction strategies: mechanical (cryocrushing, homogeneisation), chemical (oxidation and acid hydrolysis), or biological

Abbreviations: WHS, water hyacinth stems; Cel-A, Avicel® cellulose; Cel-WH, water hyacinth cellulose; CNC, cellulose nanocrystals; CNF, cellulose nanofibres; CNP, cellulose nanoparticles; CNP-BP, standard for cellulose nanocrystals; CNF-BP, standard for cellulose nanofibres; CNP-AV, cellulose nanoparticles obtained from Cel-A; CNP-WH, cellulose nanoparticles obtained from Cel-WH; SEM, scanning electron microscopy; AFM, atomic force microscopy; NTA, nanoparticle tracking analysis; XRD, X-ray diffraction; FTIR, fourier transform infrared spectroscopy

* Corresponding author at: Laboratorio de Nanotecnologia e Ingeniería Molecular, Area de Electroquimica, Depto. de Quimica, CBI, Universidad Autonoma Metropolitana-Iztapalapa, Av. San Rafael Atlixco 186, Col. Vicentina, 09340 Mexico, D.F., Mexico.

E-mail address: bani@xanum.uam.mx (N. Batina).

https://doi.org/10.1016/j.carbpol.2019.05.058
Received 21 December 2018; Received in revised form 7 May 2019; Accepted 20 May 2019
Available online 22 May 2019
0144-8617/

(enzymatic hydrolysis) (Abraham et al., 2011). Currently, commercially available CNP are isolated by chemical hydrolysis with sulphuric acid (64% w/v) to eliminate the amorphous regions (Xu et al., 2013). However, the use of sulphuric acid has several important drawbacks, such as equipment corrosion, undesirable modification of cellulose nanoparticles (surface sulphation), potential cellulose degradation, and environmental incompatibility, which complicate the handling and final disposal of the acid waste (Li, Yue, & Liu, 2012; Satyamurthy, Jain, Balasubramanya, & Vigneshwaran, 2011). Greener alternatives for the synthesis of CNP are required, and the key could be in the cellulose structure. Cellulose is composed of glucose chains linked by glycosidic bonds (ß–1→4) packed in highly-ordered regions (crystalline) alternating with disordered regions (amorphous) and embedded in a complex matrix of hemicellulose and lignin (Anderson et al., 2014). Hence, the use of enzymatic hydrolysis of cellulose through cellulase complexes could be a promising green chemistry process for the isolation of CNP due to its mild reaction conditions that do not modify the characteristics of the obtained cellulose nanoparticles. Cellulases hydrolyse the glycosidic bonds (ß–1→4) in cellulose (Chen et al., 2012); three enzyme activities act synergistically during cellulose hydrolysis: endoglucanase (EC 3.2.1.4), cellobiohydrolase (EC 3.2.1.91), and cellobiase (ß–glucosidase, EC 3.2.1.21) (Siqueira, Tapin-Lingua, Bras, da Silva Perez, & Dufresne, 2010).

The objective of the present work was to establish the optimal conditions to isolate CNP by means of a biotechnological process based on the controlled enzymatic hydrolysis (using the cellulase complex, NS22086) of cellulose obtained from water hyacinth stems (WHS) in a fast and environmentally friendly manner. The characteristics of the obtained CNP are comparable with those obtained by conventional methods (i.e., chemical hydrolysis). Moreover, the physicochemical properties (crystallinity, structure, and surface) of the obtained CNP make them suitable candidates for a wider range of applications.

2. Materials and methods

2.1. Reagents

Avicel® cellulose PH-101 (Cel-A) was purchased from Fluka Analytical, St. Louis, MO, USA. The NS22086 cellulase complex (600 U_{CMCase}/mL) marketed by Novozymes (Novozymes A/S, Bagsvaerd, Denmark) was used for enzymatic hydrolysis of cellulose. Standard cellulose nanocrystals (CNP-BP) and standard cellulose nanofibres (CNF-BP) were purchased from BioPlus (American Process Inc., GA, USA).

2.2. Harvesting of water hyacinth stems and cellulose extraction

The water hyacinths were collected from Cuemanco Lake, Xochimilco, Mexico. Only stems were used as the raw material for CNP isolation. The stems were rinsed with tap water, chopped, sun-dried until the water content was below 10%, and milled (Corona Grains Mills, Landers & Cia, USA). Cellulose (Cel-WH) was extracted from WHS following the procedures described by Pedraza-Segura, Toribio-Cuaya, and Flores-Tlacuahuac (2013) and Toribio-Cuaya et al. (2014). The obtained Cel-WH contained approximately 90% cellulose.

2.3. Enzymatic hydrolysis

The enzymatic hydrolysis of Cel-WH was conducted at 50 °C in 0.1 M citrate buffer, pH 5.0, with 10 mg/mL substrate. The cellulase complex was added at 0.12 $U_{CMCase}/mg_{Cel\text{-}WH}$. The hydrolysis reaction was stopped by boiling at 92 °C in a water bath for 15 min. The following enzymatic hydrolysis times were evaluated: 0, 15, 30, 60, 120, 240, 360, 600, and 720 min.

2.4. Isolation of cellulose nanoparticles

The solubilised cellulose fraction was separated by centrifugation (3500 rpm for 10 min). The precipitates, containing unhydrolyzed cellulose and CNP, were suspended in 0.25% w/v SDS solution and centrifuged (3500 rpm for 10 min). The precipitates were washed three times with 5 mL distilled water, sonicated at a fixed frequency of 42 kHz (Cole-Parmer, IL, USA) for 30 min, and left to settle. After 12 h, the suspended particles were recovered and assumed to be “cellulose nanoparticles (CNP)”. This procedure was repeated until the supernatants were visually transparent. Subsequently, the supernatants were collected, centrifuged (3500 rpm for 10 min), and dehydrated at 60 °C for at least 12 h (Filson, Dawson-Andoh, & Schwegler-Berry, 2009).

The obtained CNP were labelled as CNP-WH0, CNP-WH15, etc., in accordance with the enzymatic hydrolysis time. The CNP-AV120 sample was obtained following 120 min enzymatic hydrolysis of Cel-A (reference material) under the same conditions.

2.5. Released reducing sugars and glucose

The concentration of reducing sugars and glucose were measured in the supernatant following hydrolysis using the 3-5-dinitrosalicylic acid (DNS) (Miller, Blum, & Glennon, 1960) and glucose oxidase (Glucose-LQ kit, Spinreact, Girona, Spain) assays. In both cases, glucose was used as the standard.

2.6. Scanning electron microscopy (SEM)

The morphology of the fibres prior to enzymatic hydrolysis was studied by SEM. Dehydrated samples were sprinkled over a graphite film in an aluminum holder and sputtered with gold. Scanning electron microscopy (SEM) micrographs were obtained using a JSM-5900 (JEOL, Tokyo, Japan) scanning electron microscope at 2–10 kV (Flauzino Neto, Silvério, Dantas, & Pasquini, 2013).

2.7. Particle size distribution

Nanoparticle tracking analysis (NTA) was conducted using a Nanosight NS300 (Malvern Instruments Ltd, Worcestershire, U.K.) to assess the particle size distribution (PSD) of the obtained CNP. This technique uses dynamic light scattering to measure the diffusion coefficient of particles moving under Brownian motion, and converts it to the hydrodynamic diameter by the Stokes-Einstein equation (Morais, Rosa, De Souza Filho, Nascimento, & Cassales, 2013). In brief, 1 mL diluted CNP suspension (1:100 in distilled water) was introduced to a chamber, and 1-min videos were recorded and analysed using the NanoSight NTA 3.1 software (Dai, Fan, & Collins, 2013; Quevedo, Olsson, Clark, Veinot, & Tufenkji, 2014).

2.8. Atomic force microscopy (AFM)

AFM was used to determine the morphology and dimensions of CNP samples. The CNP suspensions were diluted 1:100 with ultra-pure Millipore water and homogenised by sonication for 15 min. Subsequently, 500 µL was placed on a mica holder and left to dry overnight. CNP images were generated using an atomic force microscope (NanoScope IVa, Multimode SPM, Veeco Inc., Santa Barbara, USA). All scans were obtained in air at room temperature, with commercial Si nanoprobes at a resonance frequency of 300–330 kHz. Images were collected in the tapping mode with a slow scan rate (0.5 line/s) using a J-type scanner. For quantitative measurements, each sample was evaluated in at least 20 different fields of view.

2.9. Fourier transform infrared spectroscopy (FTIR)

Structure and changes in chemical composition following enzymatic

hydrolysis were studied by FTIR. Measurements were conducted using a Spectrum GX System spectrometer (Perkin Elmer, USA) in the ATR mode. Spectra were recorded in air from 4000 to 400 cm^{-1} at 4 cm^{-1} resolution, and 16 scans were performed for each sample in the absorbance mode (Rosa et al., 2010).

2.10. X-ray diffraction (XRD)

The XRD diffractograms were collected at room temperature within a 2Θ range from 5 to 45° using a diffractometer (Krystalloflex D500, Siemens, Germany), *Kα* radiation (40 kV and 20 mA), and a wavelength of 1.5406 Å (Díaz et al., 2017).

The crystallinity index (*CrI*) was determined using the Segal method, as shown in (1):

$$CrI = \frac{I_{002} - I_{am}}{I_{002}} * 100 \quad (1)$$

Where CrI represents the relative degree of crystallinity, I_{002} is the intensity of the 002-lattice diffraction at 2Θ = 22.8°, and I_{am} is the intensity of diffraction at 2Θ = 18°. I_{002} represents both crystalline and amorphous regions, while I_{am} represents only the amorphous region (Flauzino Neto et al., 2013).

3. Results and discussion

3.1. Cel-WH extraction

The treatment used for Cel-WH extraction from WHS caused changes in fibre morphology. In the untreated WHS micrograph (Fig. 1a), each elementary fibre displays a compact structure with a smooth surface, due to the presence of certain non-fibrous compounds, and exhibits alignment in the fibre-axis direction. Following cellulose extraction (Fig. 1b), the surface became rougher. Moreover, separation of individual fibres was observed, attributable to the removal of hemicellulose and lignin, which could be favourable for the accessibility of cellulase enzymes for controlled hydrolysis of Cel-WH (Fortunati et al., 2013; Johar, Ahmad, & Dufresne, 2012). In contrast, the appearance of Cel-A, a standard material obtained from cotton linters (Fig. 1c), presents a rough surface similar to that of Cel-WH, confirming the removal of non-fibrous compounds. Cel-A has been widely reported as a source of cellulose for the isolation of nanoparticles, in addition to being a material of high purity and high crystallinity; therefore, analysing it and the nanoparticles obtained from this material (CNP-AV) allowed us to evaluate and validate the isolation method proposed in the present study.

The composition of Cel-A was 99.82% cellulose, which is in accordance with the results reported by Zhang et al. (2007) and the content declared by the manufacturer; whereas, the cellulose content of Cel-WH was 89.88%. In both cases, the content of hemicellulose was undetectable, and only traces of lignin were present. The sequential application of treatments (dewaxing and thermochemical and alkaline-peroxide treatments) for the extraction of cellulose from WHS are a feasible and environmentally friendly alternative for the removal of hemicellulose and lignin, since it leaves a material with a high cellulose concentration that is susceptible to enzymatic hydrolysis under moderate conditions of temperature and time.

3.2. Enzymatic hydrolysis of Cel-WH

Enzymatic hydrolysis carried out by cellulases preferentially hydrolyses the amorphous domains of cellulose, leaving the crystalline domains intact (Quiroz-Castañeda & Folch-Mallol, 2013). The reducing sugars and glucose released as a function of the hydrolysis time were monitored up to 720 min. The content of reducing sugars and glucose gradually increased until their maximum value was attained after 360 min (8.5 ± 0.11 mg/mL and 6.7 ± 0.19 mg/mL of reducing sugars and glucose, respectively). The amorphous domains of the cellulose were fully hydrolysed within the first 360 min of the reaction, leaving the crystalline domains free, after which the hydrolysis of the crystalline fraction began (Fig. 1d). In comparison with studies reported in the literature, our results show that the cellulase complex, NS22086, is capable of completely hydrolysing the amorphous domains of Cel-WH

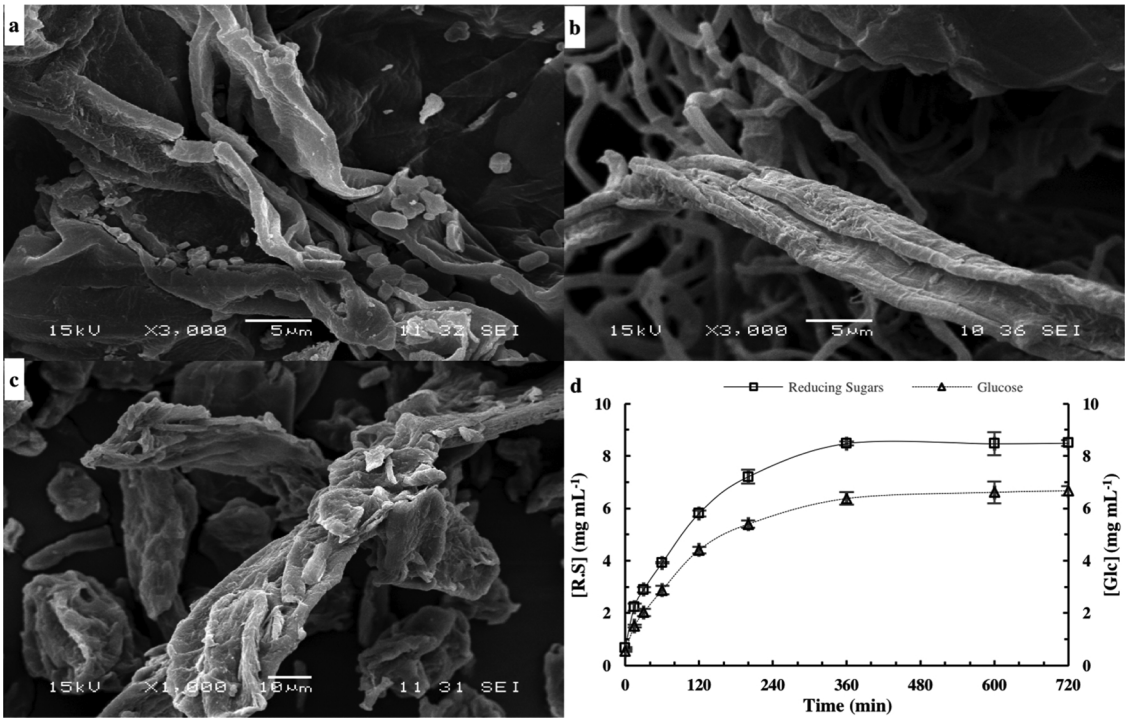

Fig. 1. SEM micrographs of (a) untreated WHS, (b) Cel-WH, (c) Cel-A, and (d) kinetics of the release of reducing sugars (R.S.) and glucose (Glc) from Cel-WH by enzymatic hydrolysis using the cellulase complex, NS22086.

in a shorter time period (˜ 6 h vs. 70–120 h) (Satyamurthy et al., 2011; Zhu, Sabo, & Luo, 2011). This finding represents a significant advantage, since the process can be customised to the desired degree of hydrolysis.

3.3. CNP isolation and measurement of particle size distribution

According to Henschen, Li, and Ek (2019)), the isolated nanoparticles from plant fibres can be classified as cellulose nanocrystals (CNC), when their length is 50–500 nm and their diameter is 3–5 nm, or as cellulose nanofibers (CNF), when their length is 500–2000 nm and their diameter is 4–20 nm. In this way, products obtained from Cel-WH and Cel-A comply with the definition of a nanoparticle, which requires that at least one of its dimensions be between 1 and 100 nm. Nanoparticle sizing is an important parameter for the adequate nanoparticle synthesis. However, sizing suspended nanoparticles can be challenging given the limitations of the available experimental techniques available in the market (Hassellöv & Kaegi, 2009). CNP samples obtained at different enzymatic reaction times were analysed by NTA, XRD, and FTIR. Commercial cellulose nanocrystals from BioPlus (CNP-BP) were used as a standard for comparison. From a reaction time of 0 to 360 min, the CNP-WH samples formed an opaque-white viscous gel suspension; however, after 360 min, the recovered CNP samples were a translucent suspension. The gradual change in appearance of the CNP suspension is likely related to the amount of released reducing sugars and glucose, indicating that the cellulose crystalline domain was hydrolysed into glucose and low-molecular weight oligomers (Morais et al., 2013).

Each CNP-WH suspension was subjected to particle size distribution analysis (Fig. 2a). In all cases, the percentage of CNP in aqueous suspensions with a particle size under 500 nm was greater than 90% (D90 in Table 1), indicating that almost the total population of particles

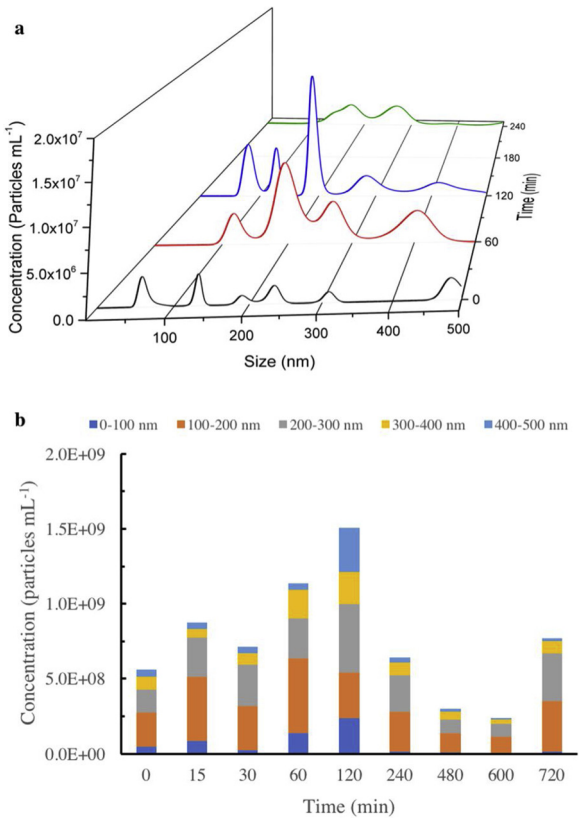

Fig. 2. (a) Particle size distribution (PSD) during the enzymatic hydrolysis process, and (b) kinetics of the particle size distribution (PSD) during the enzymatic hydrolysis process.

Table 1
Particle size distribution, 90th percentile, and crystallinity index of CNP-WH samples.

Sample	Size Particle Distribution		CrI (%)
	Mean (nm)	D90	
Cel-A			84.33 ± 0.76
CNP-AV120	190.4 ± 17.6	290.6 ± 19.9	87.76 ± 1.86
CNP-BP	219.8 ± 12.4	340.6 ± 120.9	84.78 ± 1.07
Cel-WH			*67.33 ± 0.94*
CNP-WH15	*228.1 ± 16.4*	*348.4 ± 53.9*	*62.76 ± 4.12*
CNP-WH30	*248.2 ± 20.1*	*391.9 ± 57.2*	*69.37 ± 6.32*
CNP-WH60	*252.2 ± 19.3*	*389.0 ± 25.3*	*70.74 ± 4.57*
CNP-WH120	*218.0 ± 30.5*	*378.1 ± 55.7*	*71.08 ± 7.81*
CNP-WH200	*248.3 ± 15.4*	*454.6 ± 54.0*	*67.26 ± 2.65*
CNP-WH360	*244.7 ± 21.5*	*454.5 ± 7.4*	*62.64 ± 3.05*
CNP-WH600	*294.0 ± 36.3*	*615.6 ± 127.3*	*63.33 ± 2.01*
CNP-WH720	*236.3 ± 7.5*	*320.8 ± 12.9*	*64.00 ± 1.77*

separated in the mentioned way displays sizes in the nanometric domain. At time 0 (CNP-WH0), there was a rather polydisperse distribution of CNP, with a particle size distribution (PSD) between 80 and 500 nm. This is a consequence of the cellulose extraction treatments; however, it was the lowest concentration of nanosized particles observed during the enzymatic hydrolysis process. As the hydrolysis process proceeded, the concentration of particles with a size of 120, 200, 250, and 400 nm increased significantly during the first 60 min; however, after 120 min of enzymatic hydrolysis, the maximum concentration of particles with a size of 80, 120, and 200 nm was reached, followed by a high concentration of particles with a size of 280 and 400 nm. Longer hydrolysis periods (over 240 min) led to a decrease in nanoparticle concentrations of all sizes due to the hydrolysis of the crystalline domains (Fig. 2b). These results are in accordance with the behaviour observed for the release of reducing sugars and glucose at different enzymatic hydrolysis times, in addition to the changes observed in the consistency of CNP suspensions, which demonstrates that in the range of 0–120 min of enzymatic hydrolysis of Cel-WH, the amorphous domains are hydrolysed, allowing the release of intact crystalline domains.

In all CNP samples, the average particle size (hydrodynamic diameter) was 200 to 250 nm, with a 90th percentile (D90) from 350 to 615 nm (Table 1). This is the result of a dynamic process, during which the amorphous cellulose is hydrolysed and the released crystalline cellulose accumulates until 120 min; however, afterwards, the crystalline cellulose begins to be hydrolysed, since it can be seen by the decreased concentration of nanosized particles at longer hydrolysis times. Satyamurthy et al. (2011) observed similar behaviour during the production of cellulose nanowhiskers by controlled microbial hydrolysis.

The most abundant particle size found in the CNP-WH samples at different hydrolysis times are comparable with the particle size found in the standard cellulose nanocrystals (CNP-BP), which showed an average size of 219 nm and a D90 of 340 nm (Table 1). These results are in accordance with sizes reported by other authors (Dai et al., 2013; Filson et al., 2009; Satyamurthy et al., 2011). CNP suspensions recovered from hydrolysed Cel-A (CNP-AV120) under the same conditions were different; 120 min of enzymatic hydrolysis appeared to form smaller particles, with an average size of 190 nm and a D90 of 290 nm. This could be related to the cellulose origin and the presence of different cellulose isoforms, leading to different crystal sizes (Hayashi, Kondo, & Ishihara, 2005). Therefore, based on our experimental findings, the optimal time for obtaining a high concentration of CNP-WH from WHS, at the nanoscale level with a defined structure, is 120 min.

3.4. XRD analysis

XRD analysis was performed to investigate the differences in the

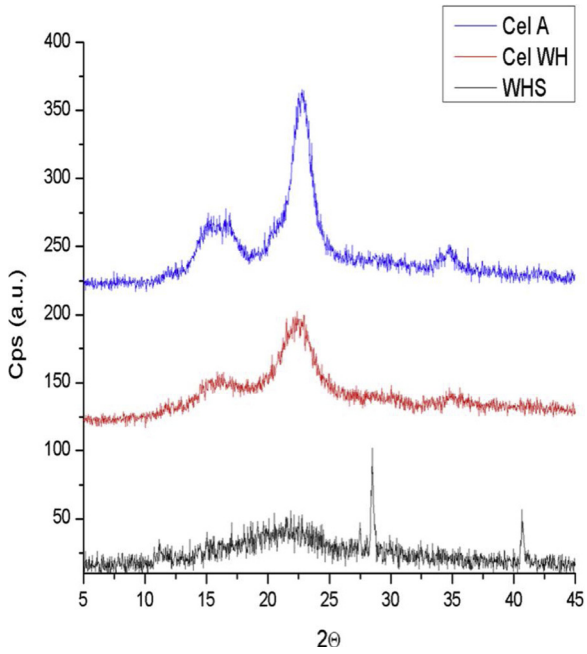

Fig. 3. X-ray diffraction patterns of the WHS, Cel-WH, and Cel-A samples.

crystalline structure between the WHS samples and Cel-WH obtained following thermochemical and alkaline-peroxide treatments (Fig. 3), in addition to the change in the crystallinity index (CrI) of the CNP obtained at different enzymatic hydrolysis times (Table 1). Cel-A (microcrystalline cellulose) was used as a reference material.

The XRD pattern of Cel-A allowed the identification of two characteristic peaks of cellulose. The first peak corresponded to the diffraction caused by the amorphous domains at 2Θ = 18°, and the second corresponded to the diffraction caused by the crystalline domains at 2Θ = 22.5°. The crystallinity index (CrI) calculated using the Segal method was ˜ 85% (Table 1). This pattern of XRD and CrI are characteristic of microcrystalline cellulose and correspond to the data reported in the literature (Abraham et al., 2013; Cherian et al., 2010). In contrast, the XRD pattern of the WHS does not show any of the characteristic peaks of cellulose, since it is a complex polymeric matrix of lignin, hemicellulose, and pectin; therefore, the proportion of cellulose is small due to the presence of all the other components in WHS. However, following extraction treatments of Cel-WH, the XRD pattern exhibits both characteristic peaks, indicating the efficient removal of lignin and hemicellulose (Abraham et al., 2013). The CrI calculated for Cel-WH was 67%, which is in agreement with the CrI reported by Flauzino Neto et al. (2013) for cellulose extracted from soybean husk (67.2%).

The CNP obtained from both Cel-WH and Cel-A (CNP-AV120) showed characteristic peaks of cellulose, but no increase in the crystallinity index was observed in the CNP from Cel-A, while the CNP obtained from Cel-WH (CNP-WH) showed a slight increase (5%) in the CrI (71%) at 120 min enzymatic hydrolysis, indicating that changes in the structure of the crystalline domains do not occur during this time. The XRD pattern of Cel-WH and CNP-WH were well defined, and after 120 min enzymatic hydrolysis, an increase of 5% was observed.

3.5. FTIR analysis

The FTIR spectra of the crude fibres of WHS, Cel-WH, and Cel-A are shown in Fig. 4a.

The peaks in the region of 3700 to 3100 cm^{-1} and 1640 cm^{-1} are observed in all spectra, but with different intensity. Both peaks are related to the stretching of hydrogen bonds and the bending of hydroxyl (OH) groups bound to the cellulose structure. The spectrum of Cel-WH shows higher intensity signals of these peaks. Moreover, all samples containing a high cellulose content show the characteristic C—H stretching vibration band around 2900 cm^{-1}. These results confirm the efficient removal of hemicellulose and lignin due to the treatments carried out during the extraction of Cel-WH from WHS (Johar et al., 2012; Mandal & Chakrabarty, 2011).

The peak at 1740 cm^{-1} in the WHS spectra corresponds to both uronic and acetyl ester bonds of ferulic and *p*-coumaric acids of lignin or hemicellulose (Thiripura Sundari & Ramesh, 2012). However, this peak disappears partially in Cel-WH following the extraction process and is not visible in Cel-A. The peak observed in all samples at 1030 cm^{-1} is likely due to the C—O—C pyranose ring (asymmetrical in the phase ring) stretching vibration. The most significant absorption band is that at 900 cm^{-1}, which is associated with the *ß*–glycosidic linkages between glucose units in cellulose. The C—C ring breathing band at ˜1155 cm^{-1} and the C—O—C glycosidic ether band at 1105 cm^{-1}, both of which arise from the polysaccharide component, are present in all spectra (Mandal & Chakrabarty, 2011).

The FTIR spectra of CNP-WH were obtained at the enzymatic hydrolysis times mentioned above. In all spectra, the characteristic peaks of cellulose (mentioned above) were identified; however, there was a variation in the intensity of the recorded peaks according to hydrolysis time (Fig. 4b). Changes in the intensity of the recorded signals are related to the energy of the hydrogen bonds between adjacent cellulose chains (Cao & Tan, 2004).

The ratio of the intensities of the peak in the region of 3440 cm^{-1} to the intensity of the peak in the region of 990 cm^{-1} ($\%T_{3440}/\%T_{990}$) has been used as an empirical measure of the hydrogen bonding intensity (HBI) and is related to the regularity of the crystalline structure of CNP and the amount of bound water (Oh, Yoo, Shin, & Seo, 2005).

From time 0–120 min enzymatic hydrolysis, no changes were observed in the HBI measured for the obtained CNP-WH, which was approximately 0.45. At longer times, a decrease in the HBI was observed (0.34) (Fig. 4c), which may be because the amorphous domains in the cellulose have been fully hydrolysed and the hydrolysis of the crystalline domains has just begun. These results coincide with the CrI measured by XRD and with the results reported by Cao and Tan (2004).

Similarly, the XRD and FTIR results show no alteration in the structure of CNP-WH fractions until 120 min enzymatic hydrolysis, since there is no significant change in the CrI, and the characteristic bands of the FTIR spectra present the same position and intensity. However, after 120 min Cel-WH enzymatic hydrolysis, a decrease in the CrI and signal intensity of the characteristic FTIR peaks was observed.

3.6. Morphological characterisation of CNP

The morphology of CNP obtained at 120 min enzymatic hydrolysis (CNP-WH120 and CNP-AV120) was evaluated by AFM. The choice was based on two aspects: *i*) the PSD analysis showed the highest concentration of nanosized particles in those cases, and *ii*) the XRD and FTIR analysis indicated a preserved crystalline structure even after 120 min enzymatic hydrolysis. The AFM image obtained for CNP-AV120 (Fig. 5a) shows the formation of a needle-shaped aggregate comprised of numerous nanocrystalline particles with an average length of 97.4 ± 14.2 nm and a diameter of 14.5 ± 2.3 nm. Nonetheless, the AFM image of the CNP-WH120 sample (Fig. 5b) reveals the presence of particles of 120.4 ± 64.4 nm in length and 22.5 ± 6.9 nm in diameter. These particles are more spread out over the substrate, well separated in the form of single nanocrystals, and exhibit less tendency to form agglomerates; therefore, the height of the particles (indication of vertical agglomeration) is very low.

The measurements show that in all the samples, at least one of their dimensions is between 1 and 100 nm; thus, they can be considered in the nanodomain (Henschen et al., 2019). AFM images of CNP-WH120 and CNP-AV120 correspond to cellulose nanoparticles denominated as “nanocrystals”, with similar characteristics to those obtained elsewhere using different cellulose sources and different hydrolysis conditions

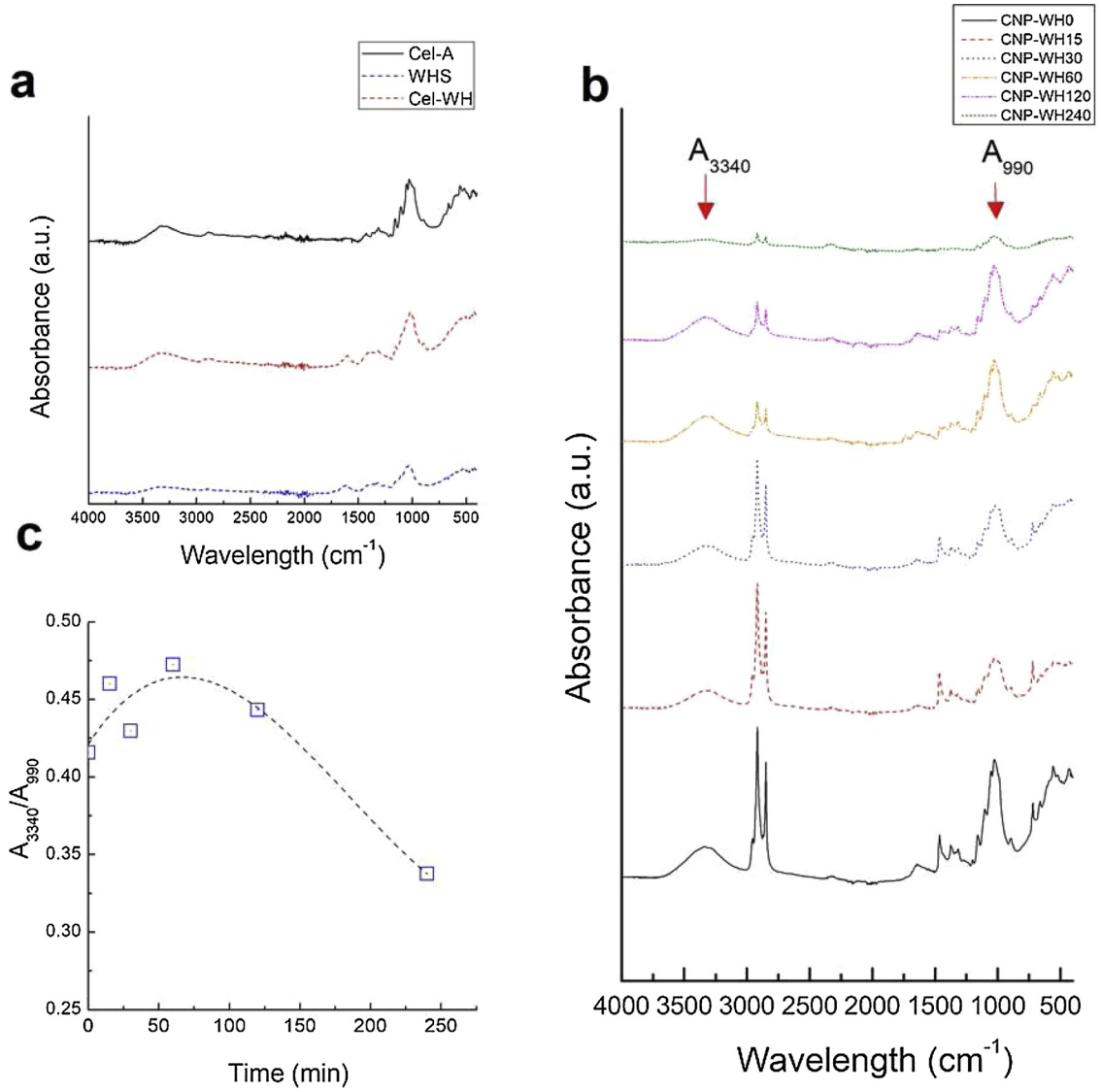

Fig. 4. (a) FTIR spectra of WHS, Cel-WH, and Cel-A samples, (b) changes in the FTIR spectra of CNP-WH as a function of the enzymatic hydrolysis time, and (c) hydrogen bonding intensity (HBI) obtained for CNP-WH samples at different enzymatic hydrolysis times.

(Cherian et al., 2010; Dai et al., 2013; Satyamurthy et al., 2011; Sèbe, Ham-pichavant, Ibarboure, Koffi, & Tingaut, 2012). Eventual differences in size, shape, and agglomeration degree are mainly due to the cellulose source (origin), extraction method, and treatments applied (Oh et al., 2005). Nominal lengths of Cel-A, CNP-WH120, CNP-AV120, cellulose nanocrystal standard (CNP-BP), and nanofiber standard (CNF-BP) are shown in Table 2. CNP-WH120 particles have a low height, small diameter, and moderate length. The AFM images also reveal that CNP-WH120 tend to remain separate without forming aggregates, while CNP-AV120 obtained under the same conditions tend to form aggregates.

AFM analysis (Table 2) also demonstrates that CNP-WH120 obtained by enzymatic hydrolysis of Cel-WH exhibit a similar size to other nanocrystalline cellulosic materials (CNP-BP and CNP-AV120). It significantly differs from the nanofibre material (CNF-BP), with a larger diameter, height, and length.

It was important to characterise the reference material using the same techniques in order to validate and observe differences in the CNP obtained according to their origin. In the present study, we observed that nanoparticles with similar characteristics were obtained (size and chemical structure); thus, the use of water hyacinth as a source of cellulose for the isolation of nanoparticles could result in a more economical and environmentally friendly process.

4. Conclusions

Application of successive thermochemical and alkaline-peroxide treatments of WHS allowed the removal of hemicellulose and lignin, releasing a cellulosic material with a high content of cellulose (˜ 90%). The amorphous domains in Cel-WH were hydrolysed enzymatically in a controlled manner in 120 min under the described experimental conditions. During this time, the maximum concentration of CNP (200–250 nm) was obtained, and also allowed cellulose nanocrystals (according to AFM analysis) to be obtained with a high crystallinity index (71%) and no changes in its structure or chemical composition according to the results obtained by XRD and FTIR analysis, respectively. Longer reaction times (> 240 min) led to the total hydrolysis of Cel-WH. AFM analysis shows that very fine CNP-WH120 nanocrystals were obtained with a diameter of 22.5 ± 6.9 nm (range 15.6–29.4 nm) and a length of 120.4 ± 64.4 nm (range 56–184.8 nm), which is very close to the nanoparticles obtained from the CNP-AV120 reference material: a diameter of 14.5 ± 2.3 nm (range 12.2–16.8 nm) and a length of 97.4 ± 14.2 nm (range 83.2–111.6 nm). Thermochemical pretreatment followed by enzymatic hydrolysis of cellulose is a novel,

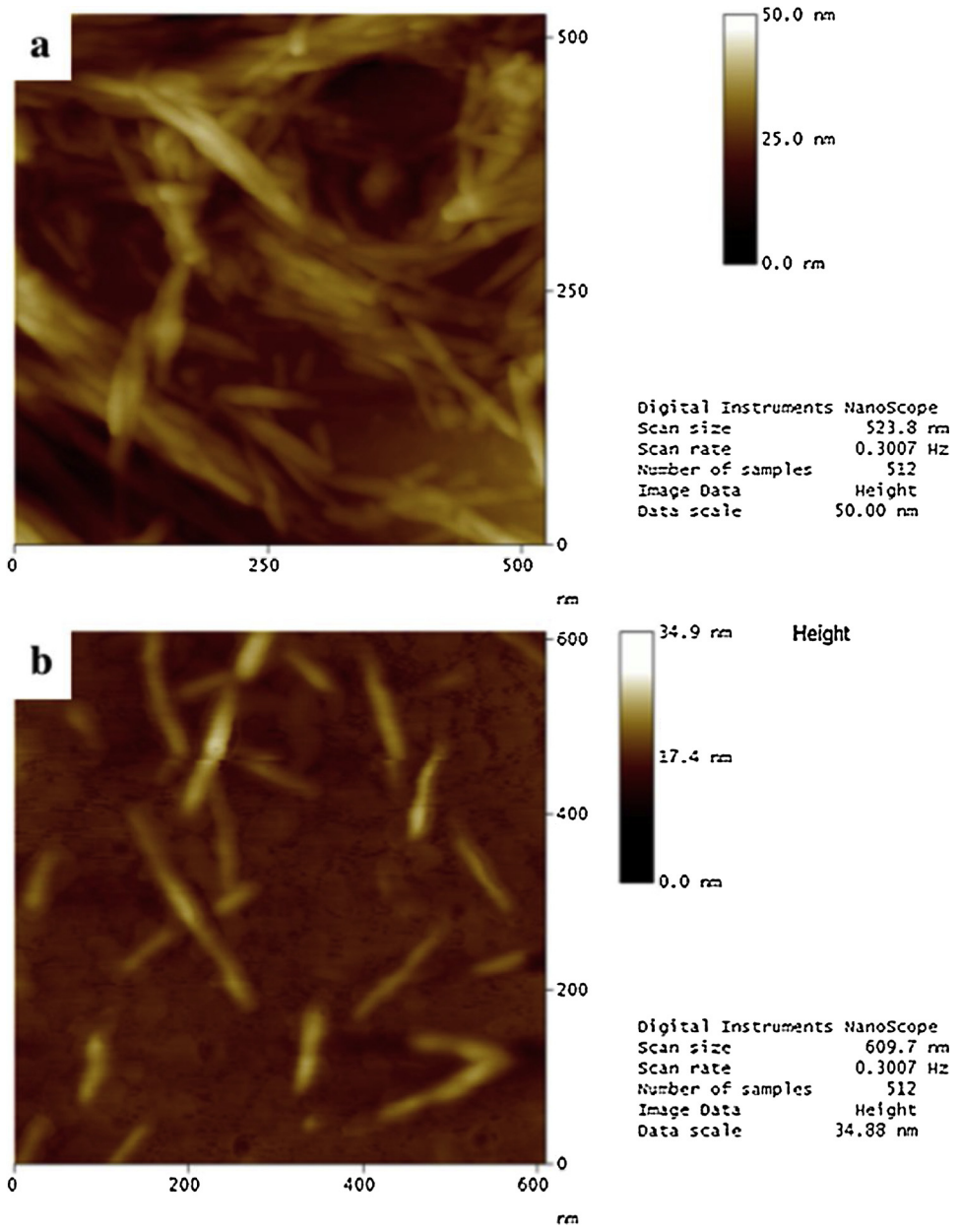

Fig. 5. (a) AFM image of the CNP-AV120 nanocrystalline sample, and (b) AFM image of the CNP-WH120 nanocrystalline sample.

Table 2
Size and dimensions obtained by AFM analysis.

Dimensions	Sample				
	Cel-A	CNF-BP	CNP-BP	CNP-AV120	CNP-WH120
Height (nm)	12.03 ± 1.99	44.82 ± 12.34	9.78 ± 1.8	5.8 ± 4.77	4.64 ± 1.79
Diameter (nm)	86.49 ± 11.35	219.06 ± 46.34	65.81 ± 14.1	14.5 ± 2.3	22.5 ± 6.9
Length (nm)	Variable, more than 1000 nm	50 – 500		97.4 ± 14.2	120.4 ± 64.4

rapid, and environmentally friendly method for the production of high-quality cellulose nanocrystals using water hyacinth stems as the raw material. Indeed, using the developed methodology, nanocrystalline cellulose of defined characteristics in terms of size, shape, crystallinity, chemical composition, and aggregation degree, can be produced under controlled conditions. The feasibility of isolating cellulose nanocrystals with defined physicochemical characteristics in a short period of time (only 120 min) has been demonstrated using an environmentally friendly method and taking advantage of the water hyacinth, which is considered a noxious weed.

Acknowledgments

We acknowledge the financial support of the Mexican Council for Science and Technology (CONACyT) through Projects No. 24711 and INFR-2016-01-270227 as well as through the postgraduate fellowship

(No. 266265) awarded to G.N.J-L., and for the Posgrado en Biotecnología (Ref. 001466). G.N.J.L. is grateful for the support of Dr. José Sepúlveda for obtaining the SEM micrographs and for the Dr. Victor Hugo Lara Corona for carrying out the X-ray diffraction analysis.

References

Abdel-Fattah, A. F., & Abdel-Naby, M. A. (2012). Pretreatment and enzymic saccharification of water hyacinth cellulose. *Carbohydrate Polymers, 87*(3), 2109–2113. https://doi.org/10.1016/j.carbpol.2011.10.033.

Abe, K., Iwamoto, S., & Yano, H. (2007). Obtaining cellulose nanofibers with a uniform width of 15 nm from wood. *Biomacromolecules, 8*, 3276–3278.

Abraham, E., Deepa, B., Pothan, L. A., Jacob, M., Thomas, S., Cvelbar, U., et al. (2011). Extraction of nanocellulose fibrils from lignocellulosic fibres: A novel approach. *Carbohydrate Polymers, 86*(4), 1468–1475. https://doi.org/10.1016/j.carbpol.2011.06.034.

Abraham, E., Deepa, B., Pothen, L. A., Cintil, J., Thomas, S., John, M. J., et al. (2013). Environmental friendly method for the extraction of coir fibre and isolation of nanofibre. *Carbohydrate Polymers, 92*(2), 1477–1483. https://doi.org/10.1016/j.carbpol.2012.10.056.

Anderson, S. R., Esposito, D., Gillette, W., Zhu, J. Y., Baxa, U., & McNeil, S. E. (2014). Enzymatic preparation of nanocrystalline and microcrystalline cellulose. *TAPPI Journal, 13*(5), 35–42.

Boluk, Y., & Danumah, C. (2014). Analysis of cellulose nanocrystal rod lengths by dynamic light scattering and electron microscopy. *Journal of Nanoparticle Research, 16*(1), 2174. https://doi.org/10.1007/s11051-013-2174-4.

Cao, Y., & Tan, H. (2004). Structural characterization of cellulose with enzymatic treatment. *Journal of Molecular Structure, 705*, 189–193. https://doi.org/10.1016/j.molstruc.2004.07.010.

Chen, X., Deng, X., Shen, W., & Jiang, L. (2012). Controlled enzymolisis preparation of nanocrystalline cellulose from pretreated cotton fibers. *BioResources, 7*(3), 4237–4248.

Cherian, B. M., Leão, A. L., de Souza, S. F., Thomas, S., Pothan, L. A., & Kottaisamy, M. (2010). Isolation of nanocellulose from pineapple leaf fibres by steam explosion. *Carbohydrate Polymers, 81*(3), 720–725. https://doi.org/10.1016/j.carbpol.2010.03.046.

Dai, D., Fan, M., & Collins, P. (2013). Fabrication of nanocelluloses from hemp fibers and their application for the reinforcement of hemp fibers. *Industrial Crops and Products, 44*, 192–199. https://doi.org/10.1016/j.indcrop.2012.11.010.

Díaz, M., Hernández, M., Ibarra, I., Guzmán, A., Lara, V., & Lima, E. (2017). Cellulose with a high fractal dimension is easily hydrolysable under acid catalysis. *Catalysts, 7*(6), 162. https://doi.org/10.3390/catal7050162.

Fattahi Meyabadi, T., Dadashian, F., Mir Mohamad Sadeghi, G., & Ebrahimi Zanjani Asl, H. (2014). Spherical cellulose nanoparticles preparation from waste cotton using a green method. *Powder Technology, 261*, 232–240. https://doi.org/10.1016/j.powtec.2014.04.039.

Filson, P. B., Dawson-Andoh, B. E., & Schwegler-Berry, D. (2009). Enzymatic-mediated production of cellulose nanocrystals from recycled pulp. *Green Chemistry, 11*(11), 1808–1814. https://doi.org/10.1039/b915746h.

Flauzino Neto, W. P., Silvério, H. A., Dantas, N. O., & Pasquini, D. (2013). Extraction and characterization of cellulose nanocrystals from agro-industrial residue - Soy hulls. *Industrial Crops and Products, 42*(1), 480–488. https://doi.org/10.1016/j.indcrop.2012.06.041.

Fortunati, E., Puglia, D., Monti, M., Peponi, L., Santulli, C., Kenny, J. M., et al. (2013). Extraction of cellulose nanocrystals from Phormium tenax fibres. *Journal of Polymers and the Environment, 21*(2), 319–328. https://doi.org/10.1007/s10924-012-0543-1.

Hassellöv, M., & Kaegi, R. (2009). Analysis and characterization of manufactured nanoparticles in aquatic environments. In J. R. Lead, & E. Smith (Eds.). *Environmental and human health impacts of nanotechnology* (pp. 211–266). Chichester, West Sussex: Wiley. https://doi.org/10.1002/9781444307504.ch6.

Hayashi, N., Kondo, T., & Ishihara, M. (2005). Enzymatically produced nano-ordered short elements containing cellulose Iβ crystalline domains. *Carbohydrate Polymers, 61*(2), 191–197. https://doi.org/10.1016/j.carbpol.2005.04.018.

Henschen, J., Li, D., & Ek, M. (2019). Preparation of cellulose nanomaterials via cellulose oxalates. *Carbohydrate Polymers, 213*(November 2018), 208–216. https://doi.org/10.1016/j.carbpol.2019.02.056.

Johar, N., Ahmad, I., & Dufresne, A. (2012). Extraction, preparation and characterization of cellulose fibres and nanocrystals from rice husk. *Industrial Crops and Products, 37*(1), 93–99. https://doi.org/10.1016/j.indcrop.2011.12.016.

Kaushik, M., & Moores, A. (2016). Review: Nanocelluloses as versatile supports for metal nanoparticles and their applications in catalysis. *Green Chemistry, 18*(3), 622–637. https://doi.org/10.1039/c5gc02500a.

Li, W., Yue, J., & Liu, S. (2012). Preparation of nanocrystalline cellulose via ultrasound and its reinforcement capability for poly(vinyl alcohol) composites. *Ultrasonics Sonochemistry, 19*(3), 479–485. https://doi.org/10.1016/j.ultsonch.2011.11.007.

Mandal, A., & Chakrabarty, D. (2011). Isolation of nanocellulose from waste sugarcane bagasse (SCB) and its characterization. *Carbohydrate Polymers, 86*(3), 1291–1299. https://doi.org/10.1016/j.carbpol.2011.06.030.

Miller, G. L., Blum, R., & Glennon, W. E. (1960). Measurement of carboxymethylcellulase activity. *Analytical Biochemistry, 2*, 127–132.

Morais, J. P. S., Rosa, M. D. F., De Souza Filho, M. D. S. M., Nascimento, L. D., Do Nascimento, D. M., & Cassales, A. R. (2013). Extraction and characterization of nanocellulose structures from raw cotton linter. *Carbohydrate Polymers, 91*(1), 229–235. https://doi.org/10.1016/j.carbpol.2012.08.010.

Oh, S. Y., Yoo, D. I., Shin, Y., & Seo, G. (2005). FTIR analysis of cellulose treated with sodium hydroxide and carbon dioxide. *Carbohydrate Research, 340*(3), 417–428. https://doi.org/10.1016/j.carres.2004.11.027.

Pedraza-Segura, L., Toribio-Cuaya, H., & Flores-Tlacuahuac, A. (2013). Multiobjective optimization approach for cellulosic biomass pretreatment. *Industrial & Engineering Chemistry Research, 52*(15), 5357–5364. https://doi.org/10.1021/ie3032058.

Quevedo, I. R., Olsson, A. L. J., Clark, R. J., Veinot, J. G. C., & Tufenkji, N. (2014). Interpreting deposition behavior of polydisperse surface-modified nanoparticles using QCM-D and sand-packed columns. *Environmental Engineering Science, 31*(7), 326–337. https://doi.org/10.1089/ees.2013.0302.

Quiroz-Castañeda, R. E., & Folch-Mallol, J. L. (2013). Hydrolysis of biomass mediated by cellulases for the production of sugars. In A. K. Chandel, & S. S. Silva (Eds.). *Sustainable degradation of lignocellulosic biomass - Techniques, applications and commercialization*InTechhttps://doi.org/10.5772/53719.

Rezania, S., Ponraj, M., Fadhil, M., Din, M. F. M., Songip, A. R., Sairan, F. M., et al. (2015). The diverse applications of water hyacinth with main focus on sustainable energy and production for new era: An overview. *Renewable and Sustainable Energy Reviews, 41*, 943–954. https://doi.org/10.1016/j.rser.2014.09.006.

Rosa, M. F., Medeiros, E. S., Malmonge, J. A., Gregorski, K. S., Wood, D. F., Mattoso, L. H. C., et al. (2010). Cellulose nanowhiskers from coconut husk fibers: Effect of preparation conditions on their thermal and morphological behavior. *Carbohydrate Polymers, 81*(1), 83–92. https://doi.org/10.1016/j.carbpol.2010.01.059.

Satyamurthy, P., Jain, P., Balasubramanya, R. H., & Vigneshwaran, N. (2011). Preparation and characterization of cellulose nanowhiskers from cotton fibres by controlled microbial hydrolysis. *Carbohydrate Polymers, 83*(1), 122–129. https://doi.org/10.1016/j.carbpol.2010.07.029.

Sèbe, G., Ham-pichavant, F., Ibarboure, E., Koffi, A. L. C., & Tingaut, P. (2012). Nanowhiskers produced by acid hydrolysis of cellulose I substrates. *Biomacromolecules, 13*, 570–578.

Sindhu, R., Binod, P., Pandey, A., Madhavan, A., Alphonsa, J. A., Vivek, N., et al. (2017). Water hyacinth a potential source for value addition: An overview. *Bioresource Technology, 230*, 152–162. https://doi.org/10.1016/j.biortech.2017.01.035.

Siqueira, G., Tapin-Lingua, S., Bras, J., da Silva Perez, D., & Dufresne, A. (2010). Morphological investigation of nanoparticles obtained from combined mechanical shearing, and enzymatic and acid hydrolysis of sisal fibers. *Cellulose, 17*, 1147–1158. https://doi.org/10.1007/s10570-010-9449-z.

Thiripura Sundari, M., & Ramesh, A. (2012). Isolation and characterization of cellulose nanofibers from the aquatic weed water hyacinth - Eichhornia crassipes. *Carbohydrate Polymers, 87*(2), 1701–1705. https://doi.org/10.1016/j.carbpol.2011.09.076.

Toribio-Cuaya, H., Pedraza-Segura, L., Macías-Bravo, S., Gonzalez-García, I., Vasquez-Medrano, R., & Favela-Torres, E. (2014). Characterization of lignocellulosic biomass using five simple steps. *Journal of Chemical, Biological, and Physical Sciences, 4*(5), 28–49.

Xu, Y., Salmi, J., Kloser, E., Perrin, F., Grosse, S., Denault, J., et al. (2013). Feasibility of nanocrystalline cellulose production by endoglucanase treatment of natural bast fibers. *Industrial Crops and Products, 51*, 381–384. https://doi.org/10.1016/j.indcrop.2013.09.029.

Zhang, Y.-H. P., Ding, S.-Y., Mielenz, J. R., Cui, J.-B., Elander, R. T., Laser, M., et al. (2007). Fractionating recalcitrant Lignocellulose at modest reaction conditions. *Biotechnology and Bioengineering, 97*(2), 214–223. https://doi.org/10.1002/bit.

Zhu, J. Y., Sabo, R., & Luo, X. (2011). Integrated production of nano-fibrillated cellulose and cellulosic biofuel (ethanol) by enzymatic fractionation of wood fibers. *Green Chemistry, 13*(5), 1339–1344. https://doi.org/10.1039/c1gc15103g.